View metadata, citation and similar papers at core.ac.uk
brought to you by CORE
provided by Institutional Repository of the Freie Universität Berlin

APPLIED PHYSICS LETTERS 107, 211901 (2015)

Enhanced absorption in tandem solar cells by applying hydrogenated In_2O_3 as electrode

Guanchao Yin,[1,a)] Alexander Steigert,[2] Phillip Manley,[1] Reiner Klenk,[2] and Martina Schmid[1,3]
[1]*Nanooptische Konzepte für die PV, Helmholtz-Zentrum Berlin für Materialien und Energie GmbH, 14109 Berlin, Germany*
[2]*Institut für Heterogene Materialsysteme, Helmholtz-Zentrum Berlin für Materialien und Energie GmbH, 14109 Berlin, Germany*
[3]*Fachbereich Physik, Freie Universität Berlin, 14195 Berlin, Germany*

(Received 11 August 2015; accepted 10 November 2015; published online 23 November 2015)

To realize the high efficiency potential of perovskite/chalcopyrite tandem solar cells in modules, hydrogenated In_2O_3 (IO:H) as electrode is investigated. IO:H with an electron mobility of 100 $cm^2 V^{-1} s^{-1}$ is demonstrated. Compared to the conventional Sn doped In_2O_3 (ITO), IO:H exhibits a decreased electron concentration and leads to almost no sub-bandgap absorption up to the wavelength of 1200 nm. Without a trade-off between transparency and lateral resistance in the IO:H electrode, the tandem cell keeps increasing in efficiency as the IO:H thickness increases and efficiencies above 22% are calculated. In contrast, the cells with ITO as electrode perform much worse due to the severe parasitic absorption in ITO. This indicates that IO:H has the potential to lead to high efficiencies, which is otherwise constrained by the parasitic absorption in conventional transparent conductive oxide electrode for tandem solar cells in modules. © *2015 AIP Publishing LLC*.
[http://dx.doi.org/10.1063/1.4936328]

Despite great progress achieved in photovoltaics in the last decades, energy from photovoltaics is still less competitive compared to the conventional fossil energy. Therefore, it is desirable to further improve the efficiencies of solar cells at low cost. Tandem solar cells are a concept exceeding the Shockley-Queisser efficiency limit of 30% without light concentration.[1] Related work has been intensively done based on various combinations of two single-junction solar cells.[2–8] However, efficiencies beyond 20% were not yet experimentally reported among thin-film tandem solar cells. The underlying challenges mainly lie in Refs. 9 and 10: (a) there is lack of high performing high-bandgap solar cells on the top; (b) sub-bandgap transparency from the top cell is poor due to parasitic absorption, which inhibits the realization of high efficiencies of the bottom cell.

The recent emergence of organic–inorganic $CH_3NH_3PbI_3$ perovskite solar cells may provide a way out of this tandem stalemate.[11–13] Organic–inorganic $CH_3NH_3PbI_3$ perovskite solar cells have achieved an efficiency above 20% up till now.[14] $CH_3NH_3PbI_3$ is the absorber and has a relatively large bandgap of 1.6 eV.[15] It also has a high absorption coefficient and exhibits a steep absorption edge and little sub-bandgap absorption.[16] All these features render the perovskite solar cell an appealing candidate for the top cell in tandem architecture. In the last two years, the perovskite/CIGSe (Si) tandem solar cells in both monolithic (two-terminal) and mechanically stacked (four-terminal) architectures have been intensively investigated, and efficiencies beyond 30% have been theoretically predicted.[9,17–22] One of the assumptions made is an excellent sub-bandgap transparency from the perovskite cell. The perovskite solar cells typically have a transparent conductive oxide (TCO) and an Au electrode. To realize semi-transparency, TCOs were recommended for replacing the typical Au electrode in a mechanically stacked architecture.[19] For a monolithic tandem structure, only the top TCO electrode is required for the top perovskite cell, also see Fig. 2(a).

We note that the conventional TCOs (e.g., In_2O_3:Sn—ITO; SnO_2:F—FTO; and ZnO:Al—AZO) inherently suffer from transparency loss, which lowers the illumination for the bottom cell. For lab-scale cells in small size, the TCO can be relatively thin since the current collection can be assisted by metal grids on top of the TCO.[23] The resulting parasitic absorption in TCO is moderate. However, when the solar cell is up-scaled to module size, the modules are generally scribed into multiple stripes of cells, which are monolithically connected without metal grids. A much thicker top TCO electrode is required to minimize the resistive loss due to the lateral transportation of current through the TCO.[23] The resulting parasitic absorption from TCO is expected to be quite serious and the potential for high efficiency can be thus restrained. The conductivity of TCOs is determined by carrier concentration as well as carrier mobility. In conventional TCOs, a higher free carrier concentration indicates a better conductivity but at the cost of sacrificing transparency. To improve transparency without compromising conductivity, a high-mobility TCO is desirable. Therefore, in this contribution, we will investigate the opto-electronic properties of high-mobility TCO. Using optical simulations, we then evaluate how much of optical benefit can be gained by applying a high-mobility TCO compared to a conventional one as the thick top electrode in a module.

We select hydrogenated In_2O_3 (IO:H)[24] as the high-mobility TCO due to the high electron mobility and ITO as the conventional in this work. Table I presents the carrier

a)Author to whom correspondence should be addressed. Email: guanchao.yin@helmholtz-berlin.de

 © 2015 AIP Publishing LLC

This article is copyrighted as indicated in the article. Reuse of AIP content is subject to the terms at: http://scitation.aip.org/termsconditions. Downloaded to IP: 134.30.32.9 On: Mon, 23 Nov 2015 19:22:01

TABLE I. Comparison of electrical parameters of ITO and an IO:H layers.

	Electron concentration N (cm^{-3})	Electron mobility μ ($cm^2/(V \times s)$)	Resistivity ρ ($\Omega \times cm$)
ITO	6.7×10^{20}	29	3.2×10^{-4}
IO:H	1.5×10^{20}	100	4.2×10^{-4}

concentration and mobility values of ITO and IO:H films obtained by Hall measurement, which are individually averaged from 3 different thicknesses (200 nm, 300 nm, 400 nm). The corresponding resistivity is then calculated. Both ITO and IO:H in Table I were prepared by Rf sputtering from ceramic target on glass substrate without intentional substrate heating. Ar was used as the working gas. For ITO, the In_2O_3/SnO_2 composition of the target is 90:10 wt. %, and the sputtering process was done at a pressure of 4×10^{-3} mbar and a power of 60 W. For IO:H, the target is pure In_2O_3. The dopant is H_2O and was introduced from a reservoir through a needle valve. The water partial pressure was adjusted to 2×10^{-5} mbar before starting the Ar_2 gas flow. The deposition was then conducted with Ar_2 at a pressure of 5×10^{-3} mbar at a power of 60 W. Afterwards, the as-deposited IO:H sample was annealed in air for around 10 min. IO:H features an electron mobility as high as 100 $cm^2\ V^{-1}\ s^{-1}$ but a much lower electron concentration compared to ITO. As a combined effect of improved electron mobility and decreased electron concentration, IO:H exhibits a resistivity in the same order as ITO. To gain insight into optical properties of ITO and I:OH, we applied an in-house software RefDex based on transfer matrix method[25] and extracted optical constants (n, k) of ITO[26] and IO:H as examples based on the measured reflection (R) and transmission (T), which are plotted in Fig. 1. R/T curves for 200 nm thick TCO layers are shown in Fig. S1 of the supplementary material.[27] To be representative, the optical constants in Fig. 1 are also averaged from 200, 300, and 400 nm thick TCO layers. From the extinction coefficient (k), IO:H exhibits a lower absorption in the full wavelength range (350–1600 nm) compared to ITO. The absorption in the short wavelengths for both ITO ($\lambda < 450$ nm) and IO:H ($\lambda < 400$ nm) is related to the inter-

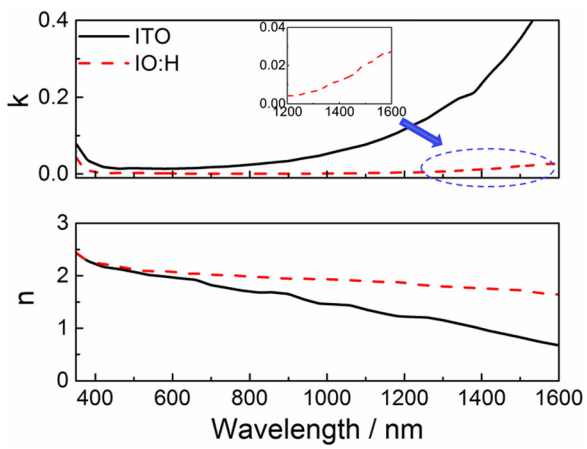

FIG. 1. Optical constants (refractive index n, extinction coefficient k) of ITO[26] and IO:H derived from transmission/reflection (R/T) via transfer-matrix method.

band transition. ITO also shows strong near infrared absorption starting from 700 nm and is gradually increasing as the wavelength increases. This is ascribed to the absorption of free carriers, which is typically observed in conventional TCOs. For IO:H, this absorption is weak, which can be mainly interpreted by the reduced electron concentration confirmed in Table I. According to the Drude model,[28] the wavelength λ of the bulk plasma frequency for free charge carriers is proportional to $1/\sqrt{N}$ (N is the free carrier concentration), the reduced electron concentration in IO:H therefore redshifts the wavelength of plasma resonance of free carriers beyond 1200 nm. For refractive index n, IO:H exhibits a moderate decreasing trend as the wavelength is increasing. ITO generally follows a similar trend but starts to drop faster from the wavelength of 700 nm, where the extinction coefficient k in ITO starts to increase.

We prepared a batch of IO:H films with varied thicknesses, all layers exhibit a high mobility (91–120 $cm^2\ V^{-1}\ s^{-1}$) and a low carrier concentration ($1.3–1.7 \times 10^{20}\ cm^{-3}$).[29] This results in a negligible parasitic sub-bandgap absorption compared to the ITO. The calculated optical constants are also similar among IO:H layers in different thicknesses. Therefore, as a good approximation, we assume that the opto-electronic properties of TCO are thickness independent and take the values in Table I and Fig. 1 as references.

To illustrate the impact of TCOs on the performance of perovskite tandem solar cell in module size, a planar monolithic architecture is proposed in this work and only the topmost TCO needs to be considered. The architecture is illustrated in Fig. 2(a) and consists of glass/EVA/TCO/C60/$CH_3NH_3PbI_3$/MoO_3/AZO/ZnO/CdS/CIGSe/Mo. Interface roughness is not taken into account. ITO and IO:H presented above are taken as top TCO electrodes. Glass and ethyl vinyl acetate (EVA) are incorporated to make the architecture comparable to the module. C60 and MoO_3 are electron and hole transporting layers,[20] respectively. Optical constants of TCOs are according to Fig. 1 and those of other layers are taken from Refs. 20, 30, and 31. The CIGSe layer has a bandgap of 1.1 eV. For the optical simulations of the tandem device, we inversely import optical constants of each layer into RefDex and calculate the reflection/transmission/absorption (R/T/Abs). For the monolithic tandem, best efficiencies are achieved when the short circuit current density of the top cell (J_{sc}^{top}) matches with that of the bottom one (J_{sc}^{bot}). In the following, all simulation results shown are thereby under the condition of matched current density J_{sc}^{match}. J_{sc} is integrated from the absorption in the perovskite and CIGSe layer without collection loss under AM 1.5 solar illumination. The typical thickness of CIGSe layer is 2–3 μm for absorbing most of the incident light. Further increasing the thickness of the CIGSe absorber will not improve J_{sc}^{match} and reducing the thickness to below 2 μm will lead to incomplete absorption and a resulting lower J_{sc}^{match}, thereby reducing the performance of the cell. For realizing the maximum efficiencies of tandem solar cells, we set the CIGSe thickness to 3 μm in this work. The thickness of the perovskite layer is varied to reach the condition of J_{sc}^{match} as the top TCO electrode changes its thickness. All other layers are constant in thickness, as shown in Fig. 2(a).

For a high performing module, the sheet resistance of the top electrode is required to be less than10 Ω/sq.[9] The TCO thickness is 320 nm for a sheet resistance of 10 Ω/sq.

This article is copyrighted as indicated in the article. Reuse of AIP content is subject to the terms at: http://scitation.aip.org/termsconditions. Downloaded to IP: 134.30.32.9 On: Mon, 23 Nov 2015 19:22:01

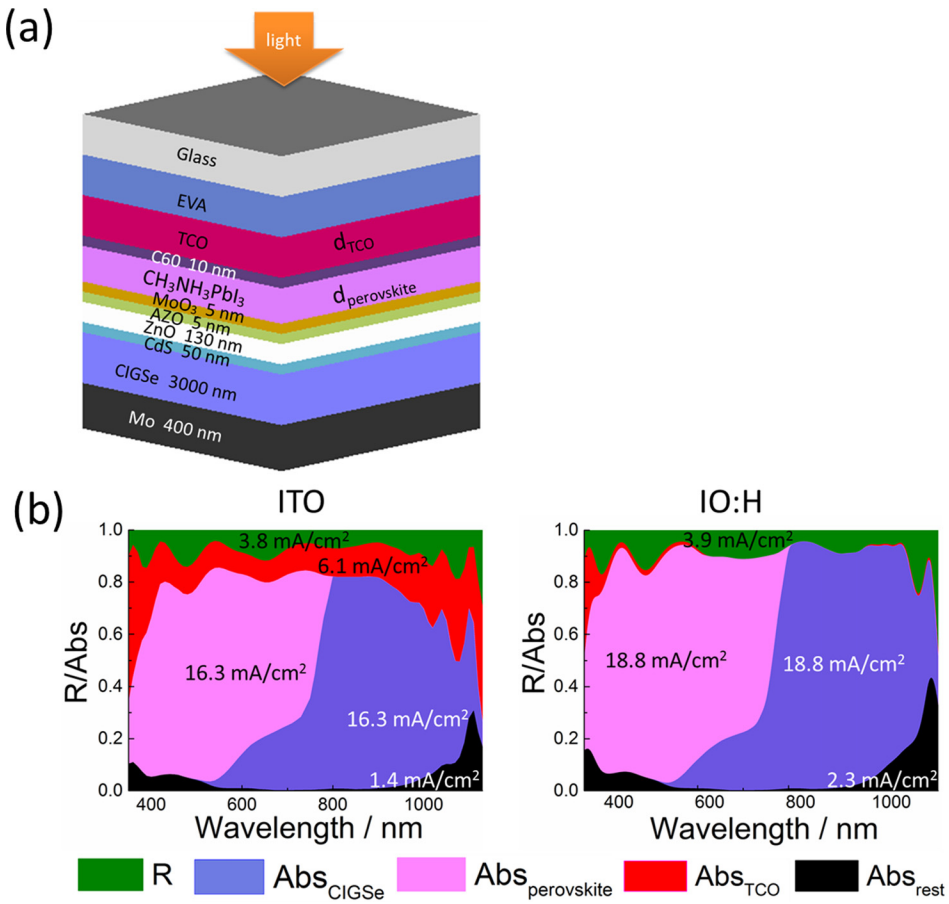

FIG. 2. (a) Schematics of device architecture of a perovskite/CIGSe monolithic tandem solar cell used for optical simulation; (b) reflection and absorption (R/Abs) of the whole tandem device with a 320 nm thick ITO (left) and IO:H (right) layer as top electrode under the condition of matched current density J_{sc}^{match} between top perovskite and bottom CIGSe cell (inset numerical values are the corresponding current densities).

Fig. 2(b) represents R/Abs of the whole tandem device with 320 nm thick ITO and IO:H as top electrode, respectively. The optical losses can be divided into 3 parts: R, parasitic absorption in TCO (Abs_{TCO}) and parasitic absorption in the rest layers (Abs_{rest}). For the tandem cell with ITO electrode, Abs_{TCO} covers the whole spectrum of interest and dominates the parasitic absorption, corresponding to a current density of 6.1 mA/cm^2 and accounting for 81.3% of the whole optical losses. In contrast to this, Abs_{TCO} is negligible for IO:H. Consequently, J_{sc}^{match} for the cell with IO:H is 2.5 mA/cm^2 higher than that for the cell with ITO. The disparity of J_{sc}^{match} between the cells with ITO and IO:H is expected to be larger as the TCO thickness increases. Fig. 3 plots the thickness of perovskite layer ($d_{perovskite}$) required for current match and the corresponding J_{sc}^{match} as a function of TCO thickness in the range of 320–1000 nm. As the ITO thickness increases, the parasitic Abs_{TCO} is increasingly severe. To reach the condition of J_{sc}^{match}, the thickness of the perovskite layer decreases to enable more light transmission into the bottom CIGSe cell. As a result, J_{sc}^{match} decreases from 16.2 to12.1 mA/cm^2 when the ITO thickness increases from 320 to 1000 nm. In contrast, for the cell with IO:H top electrode, $d_{perovskite}$ and J_{sc}^{match} are independent of the TCO thickness and keep almost constant with a value of 355 nm and 18.7 mA/cm^2 as the IO:H thickness varies. The slight fluctuations in $d_{perovskite}$ are related to the influence of interferences originating from the variations of IO:H thickness. We note here for ITO: its optical properties vary to some extent due to different deposition parameters, but the broadband absorption ability is typical.

To assess the benefit of overall performance of cells from applying IO:H as top electrode, we calculated the efficiencies of tandem cells based on a monolithic model. The equivalent circuit is illustrated in Fig. 4(a). J_{sc} is taken according to Fig. 3, and only the series resistance R_s due to the lateral transportation of current through TCO is taken into account. The photoactive width (l_1) is assumed to be 10 mm, which is reasonable for realistic module geometry. Diode 1 (D1) and diode 2 (D2) correspond to a perovskite and a CIGSe solar cell with efficiencies of 16.7%[22] and 21.7% (world record in the lab scale),[32] respectively. Their

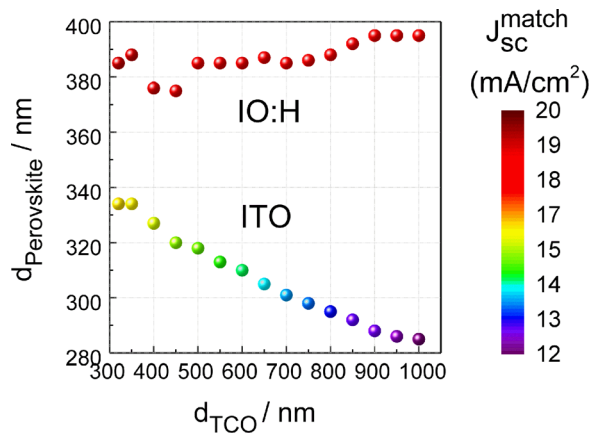

FIG. 3. Thickness of perovskite layer ($d_{perovskite}$) and the corresponding matched short circuited current density (J_{sc}^{match}) as a function of TCO thickness for perovskite/CIGSe tandem cell with ITO and IO:H as top electrode, respectively.

This article is copyrighted as indicated in the article. Reuse of AIP content is subject to the terms at: http://scitation.aip.org/termsconditions. Downloaded to IP: 134.30.32.9 On: Mon, 23 Nov 2015 19:22:01

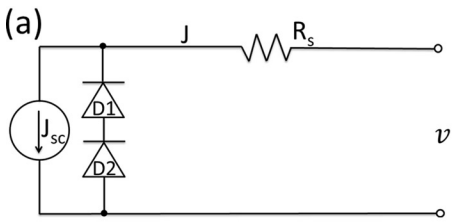

(b)

	Saturation current density J_0 (mA/cm^2)	Quality factor A	Efficiency in lab scale
Perovskite [30] D1	4.9X 10^{-7}	2.20	16.7 %
CIGSe [32] D2	2.4X 10^{-8}	1.38	21.7 %

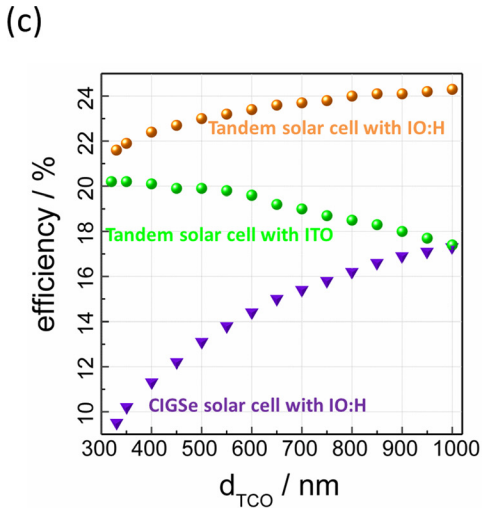

FIG. 4. (a) Equivalent circuit of the monolithic perovskite/CIGSe tandem solar cell as illustrated in Fig. 2; (b) table of diode parameters for the single-junction perovskite and CIGSe solar cell; and (c) efficiencies of perovskite/CIGSe tandem solar cells as a function of TCO thickness extracted from the model in Fig. 4(a).

diode parameters are listed in Fig. 4(b), the detailed model equations are described in supplementary material.[27] Assuming the quality of the two diodes can be maintained in the tandem structure, the $J-V$ curves of the tandem solar cell were simulated as a function of TCO thickness. The corresponding efficiencies were extracted from $J-V$ curves and are presented in Fig. 4(c). Since this is a monolithic structure, the open circuited voltage (V_{oc}) is approximately the sum of the values of the two individual single cells and is around 1.7 V. Two $J-V$ curves for the cases of ITO thickness 350 nm and IO:H thickness 1000 nm are shown in Fig. S4 in the supplementary material.[27] It should be marked here that in a realistic module several stripes of photoactive cells are monolithically connected, only one single stripe is considered for simplicity here. Nevertheless, this is enough to reflect the trend of balance between transparency and serial resistance R_s from TCO.

For the cell with IO:H as electrode, as the IO:H thickness increases, J_{sc}^{match} is constant and R_s is reducing. As a result, the efficiency remains increasing towards the ultimate value of 25.0% corresponding to the case of absence of R_s. In contrast, the efficiency for the cell with ITO is much lower, which is ascribed to the lower J_{sc}^{match} due to the parasitic absorption in ITO. The efficiency gradually decreases, though R_s is reducing. The efficiencies of the single-junction CIGSe solar cell (same geometry as the bottom cell in Fig. 2(a)) with IO:H as electrode are also calculated and are added to Fig. 4(c). We can observe that the high efficiency of 21.7% could not be maintained, which is due to the influence of lateral transport of current through TCO when cells are in module level. As expected, the CIGSe solar cell follows the similar trend as the perovskite/CIGSe tandem solar cell in efficiency as the thickness of IO:H varies. But the perovskite/CIGSe tandem solar cells outperform the single-junction CIGSe solar cells by more than 7% in efficiency, which demonstrates the benefit of tandem solar cells. Conclusively, IO:H as electrode can release the compromise between lateral resistance and parasitic absorption of TCO and thus realize high efficiencies for perovskite/CIGSe tandem solar cells in module. It should be also noted here that the highest efficiency for our perovskite tandem solar cells (around 25%) is below Shockley-Queisser efficiency limit, which was however realized in some calculations.[17–22] The main underlying reason is that different electrical models and parameters are applied.

In this study, for relaxing the compromise between transparency and resistance of conventional TCOs of tandem solar cells, we investigated the opto-electronic properties of high-mobility IO:H. The electron mobility as high as 100 cm^2 V^{-1} s^{-1} is achieved and there is almost no sub-bandgap absorption up to the wavelength of 1200 nm, which renders IO:H as an ideal electrode for solar cells. We apply IO:H as top electrode and evaluate the performance of monolithic perovskite/chalcopyrite tandem solar cells on module level, which considers lateral resistance through the TCO electrode. For comparison, ITO is taken as a reference. Due to absence of sub-bandgap absorption, J_{sc}^{match} for the cell with IO:H is significantly higher than that for the cell with ITO. Without a trade-off between transparency and lateral resistance, the tandem cell with IO:H keeps increasing in efficiency as the IO:H thickness increases and efficiencies above 21% are calculated, which is much higher than the cells with ITO as electrode. This reflects that IO:H can release the efficiency potential constrained by the parasitic absorption in conventional TCO electrode for tandem solar cells in module size.

The authors acknowledge the funding from the Helmholtz-Association for Young Investigator groups within the Initiative and Networking fund (VH-NG-928), and G. Yin specially acknowledges the support of funding from China Scholarship Council. The authors also acknowledge Hao-Wu Lin (National Tsing Hua University, Taiwan) for sharing the optical constants of C_{60}.

[1]M. A. Green, *Third Generation Photovoltaics: Advanced Solar Energy Conversion* (Springer, Berlin, Germany, 2003).
[2]A. Shah, P. Torres, R. Tscharner, N. Wyrsch, and H. Keppner, Science **285**, 692 (1999).
[3]D. Xiong and W. Chen, Front. Optoelectron **5**(4), 371 (2012).
[4]L. Dou, J. You, J. Yang, C.-C. Chen, Y. He, S. Murase, T. Moriarty, K. Emery, G. Li, and Y. Yang, Nat. Photonics **6**(3), 180 (2012).
[5]X. Wang, G. I. Koleilat, J. Tang, H. Liu, I. J. Kramer, R. Debnath, L. Brzozowski, D. A. R. Barkhouse, L. Levina, S. Hoogland, and E. H. Sargent, Nat. Photonics **5**(8), 480 (2011).
[6]W.-S. Jeong, J.-W. Lee, S. Jung, J. H. Yun, and N.-G. Park, Sol. Energy Mater. Sol. Cells **95**(12), 3419 (2011).

This article is copyrighted as indicated in the article. Reuse of AIP content is subject to the terms at: http://scitation.aip.org/termsconditions. Downloaded to IP: 134.30.32.9 On: Mon, 23 Nov 2015 19:22:01

[7]G. D. Barber, P. G. Hoertz, S.-H. A. Lee, N. M. Abrams, J. Mikulca, T. E. Mallouk, P. Liska, S. M. Zakeeruddin, M. Grätzel, A. Ho-Baillie, and M. A. Green, J. Phys. Chem. Lett. **2**(6), 581–585 (2011).
[8]J. H. Seo, D.-H. Kim, S.-H. Kwon, M. Song, M.-S. Choi, S. Y. Ryu, H. W. Lee, Y. C. Park, J.-D. Kwon, K.-S. Nam, Y. Jeong, J.-W. Kang, and C. S. Kim, Adv. Mater. **24**(33), 4523 (2012).
[9]C. D. Bailie, M. G. Christoforo, J. P. Mailoa, A. R. Bowring, E. L. Unger, W. H. Nguyen, J. Burschka, N. Pellet, J. Z. Lee, M. Grätzel, R. Noufi, T. Buonassisi, A. Salleo, and M. D. McGehee, Energy Environ. Sci. **8**, 956 (2015).
[10]M. Schmid, R. Klenk, and M. C. Lux-Steiner, Sol. Energy Mater. Sol. Cells **93**, 874 (2009).
[11]M. Liu, M. B. Johnston, and H. J. Snaith, Nature **501**, 395 (2013).
[12]A. Kojima, K. Teshima, Y. Shirai, and T. Miyasaka, J. Am. Chem. Soc. **131**, 6050 (2009).
[13]M. M. Lee, J. Teuscher, T. Miyasaka, T. N. Murakami, and H. J. Snaith, Science **338**, 643 (2012).
[14]D. A. R. Barkhouse, O. Gunawan, T. Gokmen, T. K. Todorov, and D. B. Mitzi, Prog. Photovoltaics Res. Appl. **20**, 6 (2012).
[15]J. H. Noh, S. H. Im, J. H. Heo, T. N. Mandal, and S. II Seok, Nano Lett. **13**(4), 1764 (2013).
[16]S. De Wolf, J. Holovsky, S.-J. Moon, P. Löper, B. Niesen, M. Ledinsky, F.-J. Haug, J.-H. Yum, and C. Ballif, J. Phys. Chem. Lett. **5**(6), 1035 (2014).
[17]P. Loper, B. Niesen, S. Moon, S. M. de Nicolas, J. Holovsky, Z. Remes, M. Ledinsky, F. Haug, J. Yum, S. De Wolf, and C. Ballif, IEEE J. Photovoltaics **4**, 1545 (2014).
[18]T. Todorov, T. Gershon, O. Gunawan, C. Sturdevant, and S. Guha, Appl. Phys. Lett. **105**, 173902 (2014).
[19]P. Löper, S.-J. Moon, S. Martin de Nicolas, B. Niesen, M. Ledinsky, S. Nicolay, J. Bailat, J.-H. Yum, S. De Wolf, and C. Ballif, Phys. Chem. Chem. Phys. **17**, 1619 (2015).
[20]C.-W. Chen, S.-Y. Hsiao, C.-Y. Chen, H.-W. Kang, Z.-Y. Huang, and H.-W. Lin, J. Mater. Chem. A **3**, 9152 (2015).
[21]M. Anaya, G. Lozano, M. E. Calvo, W. Zhang, M. B. Johnston, H. J. Snaith, and H. Miguez, J. Phys. Chem. Lett. **6**, 48 (2015).
[22]M. Filipič, P. Löper, B. Niesen, S. De Wolf, J. Krč, C. Ballif, and M. Topič, Opt. Express **23**, A263 (2015).
[23]K. Ellmer, A. Klein, and B. Rech, *Transparent Conductive Zinc Oxide* (Springer, Berlin, Germany, 2007).
[24]H. F. T. Koida and M. Kondo, Jpn. J. Appl. Phys., Part 2 **46**, L685 (2007).
[25]See https://www.helmholtz-berlin.de/forschung/oe/ee/nanooptix/refdex/index_en.html for Refdex introduction.
[26]G. Yin, P. Manley, and M. Schmid, J. Phys. D: Appl. Phys. **47**, 135101 (2014).
[27]See supplementary material at http://dx.doi.org/10.1063/1.4936328 for reflection and transmission of ITO and IO:H and model for a monolithic tandem solar cell.
[28]D. Ginley, H. Hosono, and D. C. Paine, *Handbook of Transparent Conductors* (Springer, Berlin, Germany, 2011).
[29]A. Steigert, I. Lauermann, T. Niesen, T. Dalibor, J. Palm, S. Körner, H. Scherg-Kurmes, R. Muydinov, B. Szyszka, and R. Klenk, Phys. Status Solidi RRL **9**, 627 (2015).
[30]P. Löper, M. Stuckelberger, B. Niesen, J. Werner, M. Filipič, S.-J. Moon, J.-H. Yum, M. Topič, S. De Wolf, and C. Ballif, J. Phys. Chem. Lett. **6**(1), 66 (2015).
[31]G. Yin, Ph.D. thesis, Technical University, Berlin, 2015.
[32]P. Jackson, D. Hariskos, R. Wuerz, O. Kiowski, A. Bauer, T. M. Friedlmeier, and M. Powalla, Phys. Status Solidi RRL **9**, 28 (2015).

This article is copyrighted as indicated in the article. Reuse of AIP content is subject to the terms at: http://scitation.aip.org/termsconditions. Downloaded to IP: 134.30.32.9 On: Mon, 23 Nov 2015 19:22:01